Fano Resonance in a Quantum Wire with a Side-coupled Quantum Dot

Kensuke Kobayashi, Hisashi Aikawa, Akira Sano, Shingo Katsumoto, and Yasuhiro Iye
Institute for Solid State Physics, University of Tokyo, 5-1-5 Kashiwanoha, Chiba 277-8581, Japan
(Dated: February 25, 2004)

We report a transport experiment on the Fano effect in a quantum connecting wire (QW) with a side-coupled quantum dot (QD). The Fano resonance occurs between the QD and the "T-shaped" junction in the wire, and the transport detects antiresonance or a forward scattered part of the wave function. While it is more difficult to tune the shape of the resonance in this geometry than in the previously reported Aharonov-Bohm-ring-type interferometer, the resonance purely consists of the coherent part of transport. Utilizing this advantage, we have quantitatively analyzed the temperature dependence of the Fano effect by including the thermal broadening and the decoherence. We have also proven that this geometry can be a useful interferometer for measuring the phase evolution of electrons at a QD.

PACS numbers: PACS numbers: 73.21.La, 85.35.-p, 73.23.Hk, 72.15.Qm

I. INTRODUCTION

The first observation of coherent transport in a mesoscopic system[1] opened up the field of electron interferometry in solids. Following the development of the Aharonov-Bohm (AB)-type interferometer, there appeared various types of electron interferometers including the Fabry-Pérot type[2] and the Mach-Zehnder type[3]. Such interferometry is of particular interest when the propagating electron experiences electronic states in a quantum dot (QD), because the interference pattern provides information on the physical properties of the QD, for example, the electron correlation inside it. Several interferometry experiments have been reported for a QD embedded in an AB ring[4–9].

In these experiments one should remember that the unitarity of electron wave propagation inevitably affects the transport property of the system. In the case of two-terminal devices, for example, this results in the phase jump of AB oscillation at the resonance[10]. While the resonance has such a subtle aspect, it brings interesting effects on the transport when it is positively used. A representative is the Fano effect[11], which appears as a result of interference between the localized state and the continuum. Although the Fano effect has been established in spectroscopy[12], its general importance in mesoscopic transport has been recognized only recently[13,14]. It has been predicted that the Fano effect appears in a QD embedded in an AB ring as schematically shown in Fig. 1 (a)[15], and recently, we have reported on its first experimental observation[16,17].

The AB geometry has an advantage such that the interference pattern can be tuned by the magnetic flux piercing the ring, while its spatial size tends to be large. In order to maintain the quantum coherence and to observe clearer effects, a smaller scale interferometer would be desirable. A candidate is the quantum wire (QW) with a finite length. A QD plus a connecting QW with measurement leads can be realized in the system schematically shown in Fig. 1 (b). Here, the very short QW connecting the QD and the lead works as a resonator. We call this geometry a "side-coupled" QD or a "T-coupled" QD.

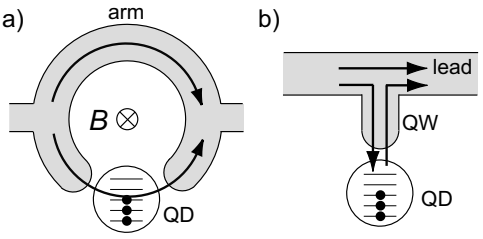

FIG. 1: (a) Schematic of a Fano system consisting of a quantum dot (QD) and an AB ring. (b) Another type of Fano system consisting of a connecting quantum wire (QW) with a "T-coupled" QD.

The essential difference between this T-type Fano system and the QD-AB-ring system studied earlier lies in the fact that the interference detects the transmitted electrons in the latter case and the reflected electrons in the former case. Hence, we can distinguish these two types of Fano effect as "reflection mode" and as "transmission mode". While the Fano effect in the reflection mode has been discussed theoretically[18–24], the experimental realization has been lacking. Furthermore, although the reflection amplitude itself conveys rich information on the QD, it has not fully been investigated since the pioneering experiment by Buks *et al*[25].

In this paper, we report on the first experimental observation of the Fano effect in a T-coupled QD. After describing the experimental setup in Sec. II, evidence for the emergence of the Fano state with decreasing temperature is given in Sec. III A. We discuss the temperature dependence of the coherence measured in this geometry in Sec. III B. Then in Sec. III C, we show that the Fano effect in a T-coupled QD can be used to detect the phase shift in the scattering by the QD, which makes it a unique tool for investigating the phase and coherence of electrons in a QD.

II. EXPERIMENT

To realize a T-coupled QD, we fabricated the device shown in the scanning electron photomicrograph of Fig. 2. It was fabricated from an AlGaAs/GaAs heterostructure by wetetching. The characteristics of the two-dimensional electron gas (2DEG) were as follows: mobility = 9×10^5 cm^2/Vs, sheet carrier density = 3.8×10^{11} cm^{-2}, and electron mean free path $l_e = 8$ μm. This device is similar to what we had previously studied[16,17]. Two sets of three fingers are Au/Ti metallic gates for controlling the local electrostatic potential. The three gates (V_L, V_g, and V_R) on the lower arm are used for defining and controlling the parameters of the QD with a geometrical area of 0.2×0.2 μm^2. The gate on the upper arm V_C is used for tuning the conductance of this arm.

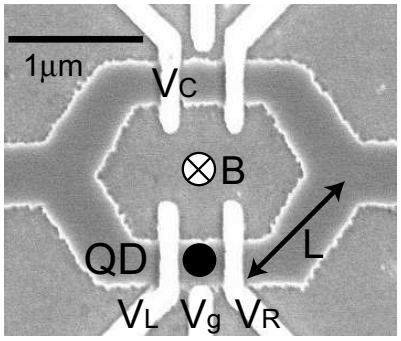

FIG. 2: Scanning electron photomicrograph of the device fabricated by wetetching the 2DEG at an AlGaAs/GaAs heterostructure. The three gates (to which voltages V_L, V_g, and V_R are applied as indicated in the figure) on the lower arm are used for controlling the QD, and the gate voltage V_C is used for tuning the conductance of the upper arm. When the gate V_L is biased strongly, the system becomes a T-coupled QD, as shown in Fig. 1 (b). The length of the QW, namely, the distance between the QD and the junction at the lead, is approximately $L \sim 1$ μm.

In the addition spectrum of the QD, the discrete energy levels inside the QD are separated by the level spacing due to the quantum confinement ΔE and the single-electron charging energy E_C. We can shift the spectrum using the center gate voltage V_g to tune any one of them to the Fermi level. In the present sample, by measuring the conductance through the QD, we found that ΔE and E_C are typically ~ 120 μeV and ~ 1 meV, respectively. We can make the device a T-coupled QD by applying a large negative voltage on V_L so that the electron transmission underneath V_L is forbidden. This is topologically the same as the T-coupled QD shown in Fig. 1 (b). The distance between the QD and the junction at the lead is $L \sim 1$ μm. When required, we made this gate slightly transmissible in order to measure the AB signal through the system with the magnetic field (B) applied perpendicular to the 2DEG.

Measurements were performed in a mixing chamber of a dilution refrigerator between 30 mK and 1 K by a standard lock-in technique in the two-terminal setup with an excitation voltage of 10 μV (80 Hz, 5 fW) between the source and the drain. Noise filters were inserted into every lead below 1 K as well as at room temperature.

III. RESULTS AND DISCUSSION

A. Emergence of the Fano Effect in the Conductance

We set V_L to -0.205 V so as to forbid the electron transmission under it. V_R was -0.190 V, which made this gate slightly transmissible. V_C was adjusted to make the conductance of the system around $2e^2/h$, which is a quasi-single channel condition. Figure 3 (a) shows typical results of the conductance through the system as a function of the gate voltage V_g at several temperatures (T). Since the connecting QW between the lead QW and the QD is narrow and long, the QD would not affect the conduction through the lead QW in the classical transport regime. Correspondingly, at high temperatures above 800 mK, hardly any characteristic structure appears in the signal. Sharp dip structures, however, rapidly grow with decreasing temperature. They are antiresonance (or reflection due to resonance) dips due to Coulomb oscillation in the QD. Furthermore, the resonant features are very asymmetric and vary widely in their line shape. For example, at $V_g = -0.485$ V and $V_g = -0.47$ V, the line shape consists of a sharp dip and an adjacent peak, while only asymmetric sharp-dip structures appear between $V_g = -0.45$ V and -0.38 V.

These line shapes in the conductance are characteristic of the Fano effect. In fact, the line shape at the lowest temperature can be fitted to[16,17]

$$G_{tot} = A\frac{(\tilde{\epsilon}+q)^2}{\tilde{\epsilon}^2+1} + G_{bg}, \tag{1}$$

where G_{bg} is the noninterfering contribution of the lead and is a smooth function of V_g that can be treated as a constant for each peak. The first term is the Fano contribution with an real asymmetric parameter q where the normalized energy

$$\tilde{\epsilon} = \frac{\epsilon-\epsilon_0}{\Gamma/2} = \frac{\alpha(V_g-V_0)}{\Gamma/2}. \tag{2}$$

The parameters A, $\epsilon_0 \equiv \alpha V_0$, and Γ represent the amplitude, the position, and the width of the Fano resonance, respectively. α is the proportionality factor which relates V_g to the electrochemical potential of the QD and is given by $\alpha = eC_g/C_{tot}$, where C_g is the capacitance between the QD and the gate V_g, and C_{tot} is the total capacitance. Note that the functional form of the Fano part in Eq. (1) can be applied to both resonance and antiresonance. The parameters of the QD can be obtained from an independent measurement of the transport through

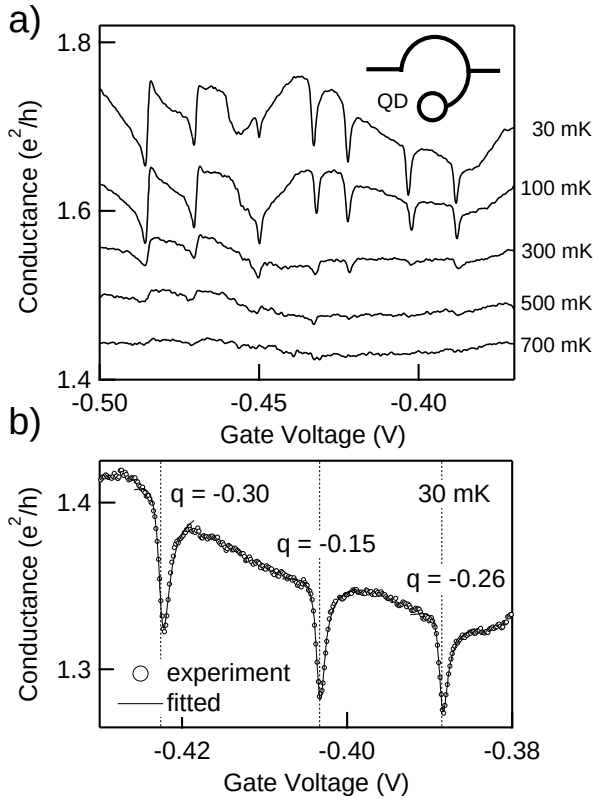

FIG. 3: (a) Conductance of the T-coupled QD as a function of V_g at several temperatures. As the temperature was lowered, the Fano feature appeared. The magnetic field was 0.80 T. The curves for $T < 700$ mK are incrementally shifted upward for clarity. (b) Three Fano features in the conductance at 30 mK are fitted to Eq. (1). The obtained q's are shown. The vertical dashed lines indicate the obtained discrete level position V_0's.

the QD under an appropriate condition of the gate voltages (applying a large negative V_C to cut the upper conduction path and opening the lower path by decreasing V_L). We estimate $\alpha = 50 \pm 10$ μeV/mV for the present system.

Figure 3 (b) shows typical results of the fitting for three dips. The satisfactory agreement assures that the Fano state is formed in the T-coupled QD system. The obtained values of Γ are ~ 70 μeV, which is much larger than the thermal broadening $3.5k_{\rm B}T = 9$ μeV at 30 mK (here, $k_{\rm B}$ is the Boltzmann constant). In Fig. 3 (b), the obtained q's are also shown and the vertical dashed lines indicate the discrete level position (V_0). Both the variation of q and that of the level spacing indicate that the conductance through this system reflects the characteristic of each of the single levels in the QD.

The data in Fig. 3 (a) is obtained at $B = 0.80$ T. The Fano effect in this system has been observed at several magnetic fields, as was also the case in the Fano effect in the QD-AB-ring system[16,17]. In the present case, the role of the magnetic field can be understood because the QW between the QD and the junction is curved as shown in Fig. 2, and the coupling is modified by the Lorentz force. In the previous reports[16,17], we have discussed that q should be a complex number in a QD-AB-ring geometry under finite B. This treatment is required to describe the V_g-B dependence of the line shape to cover the wide range of B, when the interfering phase is modulated by B. For a fixed magnetic field, Eq. (1) with a real q well describes the line shape. Furthermore in the present case, since the effective area of the connecting QW is very small, the line shape is found to be much less sensitive to the magnetic field than the case of an AB ring.

In the T-coupled geometry, the resonance is detected through the nonlocal conductance and the electric field of the modulation gate V_g works only locally, and therefore it is easy to distinguish the coherent part from the incoherent part in the conductance. In contrast, the transmission experiments such as in the QD-AB-ring system usually provide the transmission probability including both the coherent and incoherent processes[26]. For example, in the case of the Fano resonance in the AB geometry, ordinary Coulomb oscillation overlaps the coherent line shape. In the case of simple AB magnetoresistance, the magnetic field is applied all over the specimen, and the AB oscillation is superposed on the background conductance fluctuation.

B. Temperature Dependence of the Fano Effect

With increasing temperature, the dip structures are rapidly smeared out. The origins of such smearing due to finite temperature can be classified into thermal broadening and quantum decoherence. The former should be considered when $3.5k_{\rm B}T$ becomes the same order of magnitude as Γ at $T = 200$ mK. Henceforth, we focus on the thermal broadening and examine whether it alone can explain the observed diminishment of the resonance structure.

The thermal broadening appears in the distribution in $\tilde{\epsilon}$ in the Fano transmission form in Eq. (1). As noted in the previous paper[17], Eq. (1) is derived by assuming a point interaction between the localized states and the continuum. However in the present system, the length of the connecting QW is finite and dephasing during the traversal due to thermal broadening may be important. If such dephasing can be ignored, q can be treated as a real number as noted above. Conversely, the dephasing inside the connecting QW requires the use of complex q's[19].

In order to treat the thermal broadening quantitatively, we model a simple quantum circuit for the present system as shown in Fig. 4 (a). The QD is simply expressed as a tunable resonator consisting of a tunnel barrier and a perfect reflector. The phase shift of the reflector is approximated to be proportional to the gate voltage around the resonance. The connecting QW between the QD and the T-junction is simply a phase shifter of kL (k

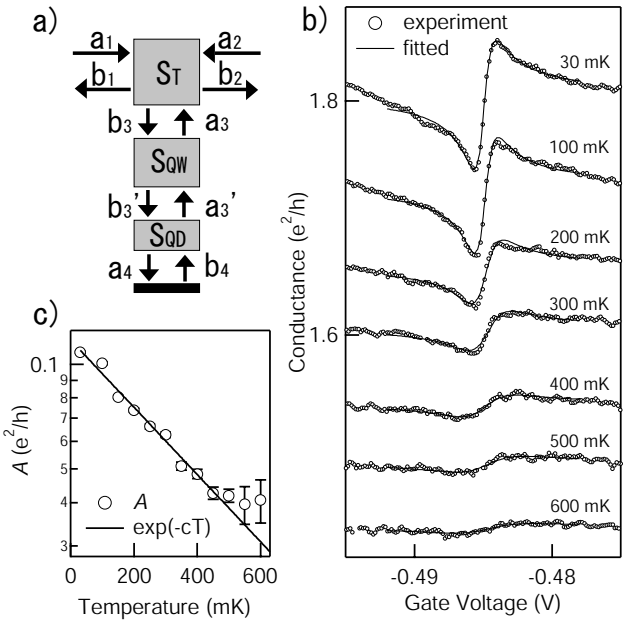

FIG. 4: (a) Model of the quantum circuit that consists of the T-junction, the QW and the QD. See also Fig. 1 (b). (b) Experimental data (open circles) and the fitted curves. The data for $T < 600$ mK are incrementally shifted upwards for clarity. (c) Obtained A value is shown in logarithmic scale as a function of temperature. The solid line shows the exponential decay $\propto \exp(-cT)$ with $c = 2.0$ K^{-1}.

: wave vector). We put the S-matrix for the junction $\boldsymbol{S}_{\rm T}$ as

$$\begin{pmatrix} b_1 \\ b_2 \\ b_3 \end{pmatrix} = \boldsymbol{S}_{\rm T} \begin{pmatrix} a_1 \\ a_2 \\ a_3 \end{pmatrix}, \quad \boldsymbol{S}_{\rm T} = \begin{pmatrix} \frac{1-a}{2} & -\frac{1+a}{2} & \sqrt{\frac{1-a^2}{2}} \\ -\frac{1+a}{2} & \frac{1-a}{2} & \sqrt{\frac{1-a^2}{2}} \\ \sqrt{\frac{1-a^2}{2}} & \sqrt{\frac{1-a^2}{2}} & a \end{pmatrix}, \tag{3}$$

to maintain the unitarity[27]. $\{a_i\}$ and $\{b_i\}$ are amplitudes of incoming and outgoing waves, as shown in Fig. 4 (a). Here, we take a as a real number, which determines the direct reflection coefficient at the junction. The S-matrix for the QW (phase shifter) is expressed as

$$\begin{pmatrix} a_3 \\ b_3' \end{pmatrix} = \boldsymbol{S}_{\rm QW} \begin{pmatrix} b_3 \\ a_3' \end{pmatrix}, \quad \boldsymbol{S}_{\rm QW} = \begin{pmatrix} 0 & e^{i\beta} \\ e^{i\beta} & 0 \end{pmatrix}, \quad \beta \equiv kL. \tag{4}$$

The S-matrix for the tunnel barrier can then be written as

$$\begin{pmatrix} a_3' \\ a_4 \end{pmatrix} = \boldsymbol{S}_{\rm QD} \begin{pmatrix} b_3' \\ b_4 \end{pmatrix}, \quad \boldsymbol{S}_{\rm QD} = \begin{pmatrix} \cos\phi & i\sin\phi \\ i\sin\phi & \cos\phi \end{pmatrix}. \tag{5}$$

Lastly, the reflector with a variable phase shift of θ is simply expressed as

$$b_4 = e^{i\theta} a_4. \tag{6}$$

By calculating the combined S-matrix, the complex transmission coefficient of the system is obtained as

$$t = \frac{1+a}{2} \cdot \frac{-1 - e^{i(\theta+2\beta)} + (e^{2i\beta} + e^{i\theta})\cos\phi}{1 + ae^{i(\theta+2\beta)} - (ae^{2i\beta} + e^{i\theta})\cos\phi}, \tag{7}$$

where

$$\beta = kL = k_{\rm F}L + \frac{L}{\hbar v_{\rm F}}(\epsilon - \mu), \tag{8}$$

since $k^2 = k_{\rm F}^2 + \frac{2m}{\hbar^2}(\epsilon - \mu)$ with $|(k - k_{\rm F})/k_{\rm F}| \ll 1$ (m : effective mass of electron). Here, μ is the position of the chemical potential and $\mu \equiv \alpha V_g$. L, $k_{\rm F}$, and the Fermi velocity $v_{\rm F}$ are estimated from the experimental conditions. The resonance of the QD occurs at $\theta = 0$, hence θ is taken as $b(\epsilon - \epsilon_0)$, where $\epsilon_0 \equiv \alpha V_0$ as in Eq. (2). It is easy to see that $|t|^2$ numerically reproduces the first term of Eq. (1) near the resonance.

The conductance of the system at the low bias ($\ll kT$) can be expressed by the Landauer-Büttiker formula as[18]

$$G_{tot} = A \int d\epsilon |t|^2 \frac{1}{4kT} \cosh^{-2}(\frac{\epsilon - \mu}{2kT}) + G_{bg}. \tag{9}$$

We treat a, b, ϕ, V_0, and G_{bg} as fitting parameters. While V_0 and G_{bg} are slightly dependent on temperature due to the neighboring Fano resonances, a, b and ϕ are treated as temperature-independent. A is left temperature-dependent to absorb decoherence other than thermal broadening.

We found that the fitting is insensitive to the value of a as long as it is smaller than ~ 0.3, which suggests that the specific form of $\boldsymbol{S}_{\rm T}$ in Eq. (3) does not affect the generality. Figure 4 (b) shows the results of the successful fitting for $a = 0$. Note that the number of crucial fitting parameters is very small since most of the parameters can be uniquely determined at the lowest temperature and taken as temperature-independent. Amplitude A is shown in Fig. 4 (c) as a function of temperature. At 600 mK, the amplitude A still remains ~ 40 % of that at the lowest temperature. The observed strong temperature dependence, therefore, is mostly due to the thermal broadening in the QW. If we set L to zero, the temperature dependence of Eq. (9) would be much weakened.

Interestingly, the behavior of A is well fitted to $\propto \exp(-cT)$ with $c = 2.0$ K^{-1} between 30 mK and 500 mK. Such temperature dependence of the coherence is reminiscent of that in an AB ring with the local and nonlocal configurations[28], where the temperature dependence of the AB amplitude was found to be weaker in the nonlocal setup than in the local setup. Theoretically it was pointed out that the difference in the impedance of the probes seen from the sample is important[29]. In the present case, since one end of the QD is cut and the nonlocal effect is observed, the impedance seen from the sample (namely, the QD and the QW connecting it to the lead) is very high and the situation is basically the nonlocal one they treated. Hence, the discussion in Ref. [29] might be applicable here. In the present case, however, we do not have the data that corresponds to the "local" setup, which can be compared with the present ones.

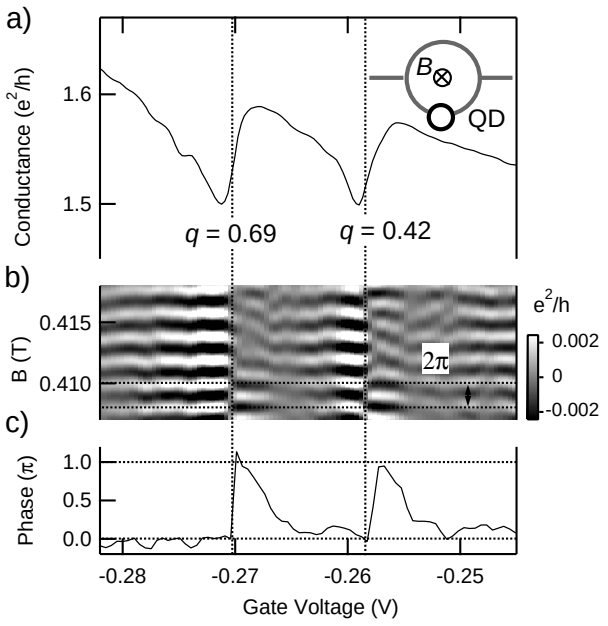

FIG. 5: (a) Two resonance dips in the conductance as a function of V_g at 30 mK at $B = 0.405$ T. The system now allows electrons to pass through the QD. The vertical lines indicate the positions of the discrete energy levels in the QD. Note that the q values are positive. (b) Gray-scale plots of the AB oscillation component of the system as a function of V_g and B. (c) Phase of the AB oscillation obtained at each V_g.

C. Phase Measurement of Electrons at a QD

Next, we discuss the application of the present geometry to the measurement of the phase evolution at the QD. While the QD-AB-ring geometry has been used for this purpose[4–9], the T-coupled QD should also provide information on the phase shift by the QD. Since in Eq. (7), the dip structure is mainly due to the resonance and phase shift in the QD, we can, in principle, extract information on the phase shift. If we restrict ourselves around the resonance point, we can utilize the simple Fano formula [Eq. (1)], instead of the complicated analysis by using the quantum circuit in the previous section. To observe this, we made the gate V_L slightly open and allowed electrons to pass through the QD. The system is now a QD-AB-ring system rather than a T-coupled QD and the Fano effect in both the reflection mode and the transmission mode is expected to occur.

Figure 5 (a) shows the conductance of the system as a function of V_g, where two resonance dips showing Fano line shape are plotted. The dashed lines indicate the positions of the discrete energy levels in the QD that are obtained by the aforementioned fitting procedure. The values of the asymmetric parameter q are given in the figure. Note that the direction of the asymmetric tail, namely, the sign of q, is the same for both dips.

Because the conduction through the lower arm is maintained very low, these Fano features change minimally with the slight variation of B, although there exists a coherent component in the transmission through the QD, which appears as a small oscillation in conductance versus B. This is the AB oscillation whose period is 2.0 mT as expected from the ring size. The AB oscillation was measured at each V_g and the AB component was extracted by fast Fourier transformation (FFT). Figure 5 (b) shows the obtained AB component in the gray-scale plot as a function of V_g and B. The coherent component through the QD is only of the order of $\sim 0.005e^2/h$, in clear contrast with the net signal up to the order of $\sim 0.08e^2/h$ [Fig. 5 (a)].

Now, we focus on the behavior of the phase of the AB oscillation. We traced the conductance maximum as a function of V_g and plotted in Fig. 5 (c) in the unit of the AB period. The phase abruptly changes by π just at the resonance points. Such a phase jump that occurs in the energy scale much smaller than Γ reflects the two-terminal nature of the present QD-AB-ring system. The AB oscillations at both dips are in-phase. This is consistent with the result of the previous report[4]. Although the origin of the in-phase nature of the Coulomb peak is still under debate despite of several theoretical studies[10,30–35], it is clear that the sign of q is the same for both dips reflecting the in-phase nature. This result, which is reproduced for other peaks in the present experiment, demonstrates that "phase measurement" can be performed simply by observing the sign of q, without investigating the AB oscillation. Interestingly, there also exists another slow π phase shift away from the resonance point commonly for these peaks, leading to their in-phase nature. Such behavior is consistent with that observed in the Fano effect in the transmission mode[16,17].

IV. CONCLUSION

We have realized the Fano effect in a QW with a side-coupled QD. The temperature dependence of the resonance structure was analyzed by including the thermal broadening, which turned out to be mostly responsible for the rapid smearing of the resonances. We have shown that the phase measurement of electrons at a QD is also possible in this geometry and gives a result consistent with that by a QD-AB-ring system. While such a simple geometry as the T-coupled QD has never been investigated experimentally, its clear advantage lies in that only a coherent signal associated with the QD is obtained. This work proves that the Fano effect in this interferometer can be a powerful tool for measuring the coherence and phase of electrons.

ACKNOWLEDGMENTS

We thank F. B. Anders, M. Eto, T. Ihn, J. König, and A. Schiller for helpful comments. This work is supported by a Grant-in-Aid for Scientific Research and by

a Grant-in-Aid for COE Research ("Quantum Dot and Its Application") from the Ministry of Education, Culture, Sports, Science, and Technology of Japan. K.K. is supported by a Grant-in-Aid for Young Scientists (B) (No. 14740186) from Japan Society for the Promotion of Science.

[1] R. A. Webb, S. Washburn, C. P. Umbach, and R. B. Laibowitz, Phys. Rev. Lett. **54,** 2696 (1985).
[2] C. G. Smith, M. Pepper, H. Ahmed, J. E. F. Frost, D. G. Hasko, R. Newbury, D. C. Peacock, D. A. Ritchie, and G. A. C. Jones, J. Phys.: Condensed Matter **1**, 9035 (1989).
[3] Y. Ji, Y. Chung, D. Sprinzak, M. Heiblum, D. Mahalu, and H. Shtrikman, Nature **422,** 415 (2003).
[4] A. Yacoby, M. Heiblum, D. Mahalu, and H. Shtrikman, Phys. Rev. Lett. **74,** 4047 (1995).
[5] S. Katsumoto and A. Endo, J. Phys. Soc. Jpn. **65**, 4086 (1996).
[6] R. Schuster, E. Buks, M. Heiblum, D. Mahalu, V. Umansky, and H. Shtrikman, Nature **385,** 417 (1997).
[7] W. G. van der Wiel, S. De Franceschi, T. Fujisawa, J. M. Elzerman, S. Tarucha, and L. P. Kouwenhoven, Science **289,** 2105 (2000).
[8] Y. Ji, M. Heiblum, D. Sprinzak, D. Mahalu, and H. Shtrikman, Science **290,** 779 (2000).
[9] Y. Ji, M. Heiblum, and H. Shtrikman, Phys. Rev. Lett. **88,** 076601 (2002).
[10] A. L. Yeyati and M. Büttiker, Phys. Rev. B **52,** 14360 (1995).
[11] U. Fano, Phys. Rev. **124,** 1866 (1961).
[12] For example, U. Fano and A. R. P. Rau, *Atomic Collisions and Spectra* (Academic Press, Orland, 1986); F. Cerdeira, T. A. Fjeldly, and M. Cardona, Phys. Rev. B **8,** 4734 (1973); J. Faist, F. Capasso, C. Sirtori, K. W. West, and L. N. Pfeiffer, Nature **390,** 589 (1997).
[13] E. Tekman and P. F. Bagwell, Phys. Rev. B **48,** 2553 (1993).
[14] J. U. Nöckel and A. D. Stone, Phys. Rev. B **50,** 17415 (1994).
[15] P. Singha Deo and A. M. Jayannavar, Mod. Phys. Lett. B **10,** 787 (1996); P. Singha Deo, Solid St. Commun. **107,** 69 (1998); C.-M. Ryu and S. Y. Cho, Phys. Rev. B **58,** 3572 (1998); K. Kang, Phys. Rev. B **59,** 4608 (1999); O. Entin-Wohlman, A. Aharony, Y. Imry, and Y. Levinson, J. Low Temp. Phys. **126,** 1251 (2002); W. Hofstetter, J. König, and H. Schoeller, Phys. Rev. Lett. **87,** 156803 (2001); Tae-Suk Kim, Sam Young Cho, Chul Koo Kim, and Chang-Mo Ryu, Phys. Rev. B **65,** 245307 (2002).
[16] K. Kobayashi, H. Aikawa, S. Katsumoto, and Y. Iye, Phys. Rev. Lett. **88,** 256806 (2002).
[17] K. Kobayashi, H. Aikawa, S. Katsumoto, and Y. Iye, Phys. Rev. B. **68,** 235304 (2003).
[18] Kicheon Kang, Sam Young Cho, Ju-Jin Kim, and Sung-Chul Shin, Phys. Rev. B **63,** 113304 (2001).
[19] A. A. Clerk, X. Waintal, and P. W. Brouwer, Phys. Rev. Lett. **86,** 4636 (2001).
[20] Maria A. Davidovich, E. V. Anda, C. A. Busser, and G. Chiappe, Phys. Rev. B **65,** 233310 (2002).
[21] A. A. Aligia and C. R. Proetto, Phys. Rev. B **65,** 165305 (2002).
[22] M. E. Torio, K. Hallberg, A. H. Ceccatto, and C. R. Proetto, Phys. Rev. B **65,** 085302 (2002).
[23] R. Franco, M. S. Figueira, and E. V. Anda, Phys. Rev. B **67,** 155301 (2003).
[24] R. M. Konik, cond-mat/0207622 (2002).
[25] E. Buks, R. Schuster, M. Heiblum, D. Mahalu, V. Umansky, and H. Shtrikman, Phys. Rev. Lett. **77,** 4664 (1996).
[26] For example, H. Aikawa, K. Kobayashi, A. Sano, S. Katsumoto, and Y. Iye, cond-mat/0309084 (2003).
[27] M. Büttiker, Y. Imry, and M. Ya. Azbel, Phys. Rev. A **30,** 1982 (1984); Björn Kubala and Jürgen König, Phys. Rev. B **67,** 205303 (2003).
[28] K. Kobayashi, H. Aikawa, S. Katsumoto, and Y. Iye, J. Phys. Soc. Jpn. **71,** L2094 (2002).
[29] G. Seelig, S. Pilgram, A. N. Jordan, and M. Büttiker, Phys. Rev. B **68**, R161310 (2003); See also G. Seelig and M. Büttiker, Phys. Rev. B **64,** 245313 (2001).
[30] C. Bruder, R. Fazio, and H. Schoeller, Phys. Rev. Lett. **76,** 114 (1996).
[31] Y. Oreg and Y. Gefen, Phys. Rev. B **55,** 13726 (1997).
[32] J. Wu, B.-L. Gu, H. Chen, W. Duan, and Y. Kawazoe, Phys. Rev. Lett. **80,** 1952 (1998).
[33] G. Hackenbroich and H. Weidenmüller, Europhys. Lett. **38,** 129 (1997).
[34] H.-W. Lee, Phys. Rev. Lett. **82,** 2358 (1999).
[35] T. Taniguchi and M. Büttiker, Phys. Rev. B **60,** 13814 (1999).